



Review

Stress corrosion cracking of pipeline steels in near-neutral pH solutions: the role of mechanochemical and chemomechanical effects

Roman I. Bogdanov¹, Yaakov B. Unigovski^{2,*}, Emmanuel M. Gutman², Iliya V. Ryakhovskikh¹ and Roni Z. Shneck²

¹ Institute of Natural Gases and Gas Technologies–Gazprom VNIIGAZ LLC, Moscow Oblast, Razvilka Settlement, Russia

² Dept. of Materials Engineering, Ben-Gurion University of the Negev, Beer-Sheva, Israel

* **Correspondence:** Email: yakovun@bgu.ac.il; Telefax: +97286461478.

Abstract: The review presents brief theoretical foundations of the mechanochemical and chemomechanical surface effects (MCE and CME) associated with corrosion-mechanical destruction of metals, considers the results of various scientific publications that studied the mechanochemical behavior of steels in near-neutral pH media, and analyzes the application of the results of such studies with the purpose of their practical use in the stress corrosion cracking (SCC) prevention. The article attempts to summarize the results of modern experimental studies and numerical modeling of mechanochemical and chemomechanical processes occurring on the surface of pipe steels and at the tip of the crack under the simultaneous effects of stresses/strains and corrosion media. The influence of these processes on the mechanism and kinetics of corrosion cracking of pipe steels in near-neutral aqueous solutions is discussed. The criteria for the quantitative assessment of the influence of MCE and CME on the SCC of pipeline steels are considered. The analysis of research methods for the study of MCE and CME, was carried out with the aim of further developing a unified methodological approach to assessment and quantification in predicting SCC in neutral media.

Keywords: near-neutral pH SCC (NNpHSCC); pipeline; mechanochemical; chemomechanical effects

1. Introduction

Stress corrosion cracking of pipeline steels is one of the most important problems in countries that have an extensive system of high-pressure buried gas pipelines. Cases of SCC of pipeline steels were reported in USA, Australia, Canada, Russia, Iran and a number of other countries [1–12]. Analysis of the literature data showed that failures of the SCC occur in gas pipelines operating in different continents and in climatic regions, built of pipes of different diameters, and, according to the standards of different countries, pipe steels had significantly different chemical composition and mechanical properties; the only constant condition for the development of this process was the access of the aqueous medium to the surface of the metal of the pipes due to disbondment of the tape coating [1,2,5,6,9,12,13].

Depending on the composition of the electrolyte under the coating, two main types of SCC of pipeline steels are distinguished: intergranular cracking in concentrated carbonate electrolytes with high pH (8–10) and transgranular cracking in dilute electrolytes with near-neutral pH (5.5–7.5). The qualitative characteristics of the main types of SCC are presented in a large number of original works and reviews [1,4–6,8,13,14].

To date, it has become apparent that it is impossible to apply the equations (or criteria) of electrochemistry and fracture mechanics separately to describe the kinetics of the SCC pipeline steels, since the process occurs under the simultaneous action of electrochemical and mechanical factors. Secondly, the mathematical (quantitative) description of the SCC models of pipeline steels is possible based on the results of experimental modelling of various stages, but the disadvantage is that the obtained empirical coefficients and dependencies cannot be used for a wide range of pipes laid in soils with different component composition.

It seems that a more realistic approach today is to divide of SCC pipeline steels into separate significant phenomena and study these phenomena separately with using of the results to improve the accuracy of the predictive SCC models of pipeline steels [15,16]. This approach allows us to describe the SCC process, but quantifying requires a more detailed study of individual effects. This will improve the accuracy of predictive SCC models of pipeline steels.

The fundamental relationships, including thermodynamics and kinetics of interactions between the chemical reactivity of a solid surface and the stress state of the surface layers, are described in [17] and further in monographs [18–21]. The acceleration of chemical reactions by mechanical action (mechanochemical effect-MCE) and the increase in near-surface plasticity caused by chemical reactions (chemomechanical effect-CME) simultaneously open up new possibilities for controlling a wide range of processes from corrosion protection to design new materials. In our opinion, such significant phenomena as mechanochemical and chemomechanical effects, which develop at the tip of stress-corrosion cracks with a synergistic interaction between them, should be more deeply investigated to prevent the failure of main gas pipelines. In the following subsections of the review, the authors will try to critically consider the use of mechanochemical methods for studying corrosion under the stress of main gas pipelines and predicting their durability in near-neutral groundwater.

2. Theoretical background and experimental verifications of MCE and CME

The term “mechanochemistry” was introduced by Wilhelm Ostwald [22] at the beginning of the XX century. The effect of mechanical deformation of a solid on the course of chemical reactions is

one of the oldest empirical observable facts, e.g., in procuring fire. Although some separate manifestations of heterogeneous mechanical actions on chemical reactions have been studied for many years, it was only in recent decades the mechanochemistry of solids began to develop as an independent science [19,23–28]. In a number of papers [29–32], the MCE is designated as M-E effect (mechano-electrochemical effect), but since the authors used the analytical dependences of the effect derived in [17–19], we will use its former name in this article. The chemomechanical effect [17–21] is the change in the physico-mechanical properties of a metal under the influence of chemical (electrochemical) reactions on its surface. In the literature, this effect is paid less attention than the opposite effect—the influence of mechanical effects on the course of chemical transformations in materials (MCE), which is due to the wide area of its practical applications. At the same time, both CME and MCE can be regarded as interrelated. The main cause of the chemomechanical effect is an increase in the flow of dislocations in the surface metal layer under conditions of chemical reactions on the surface, which causes plasticization and additional deformation of the dissolving metal. An additional flow of dislocations is formed as a result of the rapid saturation of the surface layer of the metal with dislocations to the maximum possible “dynamic” density with the subsequent removal of this layer due to chemical dissolution [19].

An ideal ordered surface of a crystalline solid does not occur in reality. Each real surface always contains a certain number of structural defects. Steps between adjacent crystal planes constitute one of the most common structural surface defects. Zero-dimensional or point defects include adatoms, vacancies, and dislocation emergence points on the terrace; kinks, step adatoms, as well as step vacancies at steps. One-dimensional or line defects involve step edges and domain boundaries [33]. At the surface, the main kinetically stable defects are points of dislocation emergence, meanwhile in the crystal bulk the dislocations are line defects. At the point of dislocation emergence, the ordering of the surface atoms is disrupted. The emergence of a screw dislocation creates a step, which is tied at one end to the dislocation emergence point. There may be other sources of steps on the surface, which overwhelm the effect of dislocations, such crystal edges, point defects, particularly impurities, as well as unassisted nucleation of steps in the unstrained regions between the dislocations [33].

Up-to-date concepts of the dissolution of a crystalline solid (e.g., anodic dissolution mechanism of metals) are based on the idea of the initial formation of monatomic pits (bidimensional dissolution nucleus) and sequential etching of atomic layers along the crystallographic plane by shifting the monatomic step with successive repeating of the layer dissolution process. The surfaces of monatomic steps may also serve as sources of new dislocations [19]. Therefore we can conclude that the appearance of an additional flux of dislocations due to the dissolution of surface atoms by the anodic current (CME) is caused by heterogeneous nucleation and the action of new surface sources of dislocation with formation of monatomic steps [19,34]. The saturation of dissolving layer with dislocations is possible because of the very high (almost sonic) velocity of dislocation multiplication as compared to solid dissolution, which take a few second to etch one monatomic layer. Thus, favourable conditions are created for multiple slip dislocations and, consequently, for relaxation of microstresses and a decrease in the hardness of the surface layer [19].

In accordance to the mechanochemical theory, a stressed solid (working electrode) dissolving in an electrolyte changes its equilibrium electrode potential due to the mechanical stress. The decrease in the equilibrium electrode potential $\Delta\varphi_0$, corresponds to an increase in mechanochemical activity and a decrease in corrosion resistance of a solid. The value $\Delta\varphi_0$ for a solid system of positive ions due to the presence of the mechanical action of positive or negative elastic stresses (their

absolute value $\Delta P > 0$) and plastic deformations of a solid can be found from Eqs 1 and 2, respectively [19]:

$$\Delta\varphi_0 = - \frac{\Delta P V_m}{zF} \quad (1)$$

$$\Delta\varphi_0 = - \frac{n\Delta\tau R}{\bar{\alpha} k N_m z F} \quad (2)$$

where V_m —molar volume; z —charge-transfer valence; F —Faraday constant; n —number of planar dislocations in a pile-up; τ —resolved shear stress; R —universal gas constant; $\bar{\alpha}$ —coefficient, describing mobile dislocation density (10^9 – 10^{11} cm^{-2}); k —Boltzmann's constant and N_m —maximum possible dislocation density considered as one mole of dislocations.

The anodic current increase Δi_a can be expressed by the Eqs 3 and 4 [19]:

$$\Delta i_a = i_a \left[\exp\left(\frac{n\Delta\tau}{\bar{\alpha} k T N_m}\right) - 1 \right] \quad (3)$$

where i_a is the anodic current density before plastic deformation at the same anodic potential.

In the dynamic regime of plastic flow, the magnitude of MCE depends on the deformation rate $\dot{\epsilon}$ defining hardening magnitude:

$$\Delta i_a = i_a \left(\frac{\dot{\epsilon}}{\dot{\epsilon}_0} - 1 \right) \quad (4)$$

where i_a^0 is the anodic current density for the strain rate $\dot{\epsilon}_0$, T is the temperature.

As experimental verification of MCE, it was investigated the effect of plastic strain on kinetics of cathodic and anodic processes on wire specimens of low-carbon steel [17–19]. As can be seen from Figure 1 [19], the increase in anodic increment Δi_a before the onset of easy glide is proportional to the growth of strain hardening $\Delta\tau$ in the stress range between the elastic limit and the beginning of easy glide. Summing up the theoretical analysis of the effect of plastic deformation on MCE, we should point out three stage of strain hardening curve. In the stage I—new dislocations appear at easy glide without planar pile-ups formation. MCE does not increase essentially and may even decrease due to relaxation of existing pile-ups. Besides, a small mechanochemical activity at initial stage of plastic deformation is due to the pinning of the motion of the originally existed dislocations by Cottrell atmospheres-atoms of carbon or nitrogen [35]. Stage II is characterized by intense strain hardening at the stress increase, and planar pile-ups appear leading to sharp increase in MCE in accordance with Eq 2. Dislocation glides and cross slips lead to their uneven distribution, resulting into numerous dislocation tangle and pile-up groups that collectively contribute to the strain-hardening of the polycrystalline metal [36]. Stage III as a final stage of dynamic recovery is characterized by planar pile-ups destroying, cell walls (sub-boundary) are formed leading to the sharp decrease in n values (Eq 2), strain hardening is weakened, and MCE significantly decreases.

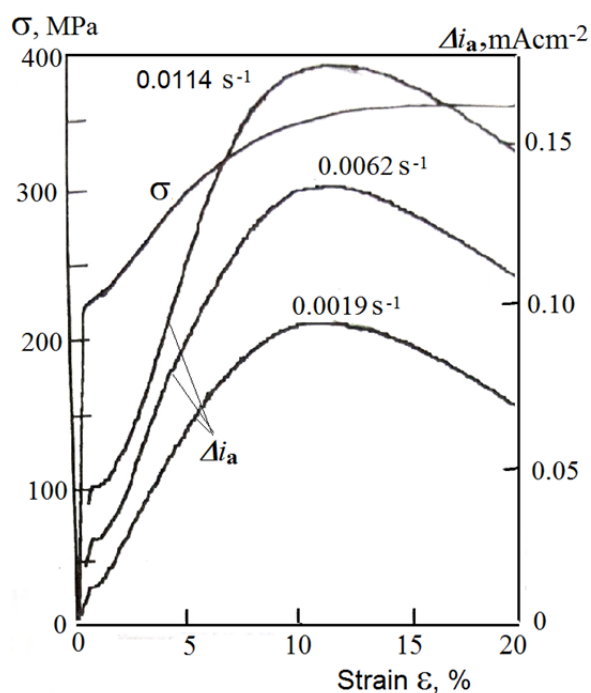


Figure 1. The effect of strain and strain rate $\dot{\epsilon}$ on anodic current density i_a for low-carbon wire steel in 3.5 M H_2SO_4 (Reprinted with permission from Ref. [19]).

To study the chemomechanical effect on the metal surface, various electrochemical, physical and mechanical methods were used, such as measuring nano- and micro-hardness under conditions of anodic polarization [19,37–39]. Experiments conducted on iron single crystals and steels confirmed the presence of the chemomechanical effect in microhardness tests [19]. A linear dependence of the hardness loss on the logarithm of the current density in all ranges of passive potentials is established for 304-type stainless steel in a solution of 3.5M H_2SO_4 . Recently, this effect was also confirmed for carbon and silicon steels, where the change in steel hardness was associated with a depth of the surface layer of 10–25 μm [38]. The relative microhardness of AISI 1070 steel derived as the square ratio of penetration depth of an indenter in air and in 0.6M NaCl solution $(\Delta h_{air}/\Delta h_{sol})^2$ show the minimum (noticeable CME) at near-neutral pH values. Explaining this finding requires further study. The reduction of the nano-hardness under anodic polarization comparing to air was confirmed also for pure iron [37] and for Cr–Ni 800 alloy [39]. The locally increased ductility of metals due to anodic dissolution (CME) causes a creep rate jump compared to that in air, e.g., for copper in acetic acid [40], 316L stainless steel in MgCl [41], Mg and Mg–Al alloys in the buffer and NaCl solutions [42–43]. Additionally, elongation of a high-strength Cr–Ni–V alloy with anodic polarization in 0.5 M H_2SO_4 sulfuric acid is approximately 40% more than that obtained in air [21].

The role of MCE in SCC of metals has been undoubtedly established, e.g., by Hoar for stainless steels where it was found that “yield-assisted anodic dissolution of 18-8 chromium-nickel steel is clearly a conjoint mechano-chemical phenomenon, not the result of consecutive action of separate mechanical and chemical processes” [44]. Additionally, it was found [45–46] that the effect of yielding (plastic deformation) on the rate of the anodic dissolution of metals (Fe, Mo, Ni, and Cu) in acid solutions is much more pronounced than that of the elastic deformation. It can be assumed that MCE plays a very important role not only in accelerating the rate of anodic dissolution and

nucleation of cracks from corrosion pits, but also in increasing the propagation velocity of cracks in such a complex multi-stage process as SCC. To explain the SCC phenomenon scientifically, many different mechanisms or models have been proposed. So far, numerous researchers, such as Scully [47], Ford and Andresen [48], Parkins [4,49], Saito & Kuniya [50], have associated corrosion cracking with film formation and destruction at the tip of growing crack, i.e., with active-to-passive transitions.

As stated by Saito & Kuniya [50], they present “a predictive methodology for SCC crack growth using a mechanochemical model based on slip formation/dissolution mechanism”. However, this is actually not a mechanochemical model, and it is based only on the Ford–Andresen (FA) film rupture-dissolution model [48], which was supplemented by the known parameters of plastic deformation at the crack tip. With this limited approach, anodic dissolution at the crack tip was taken into account only for the bare surface generated as a result of the formation of active planes due to plastic deformation. In the equations presented by the authors, the crack growth rate is related to the average current density of the anodic dissolution, which is defined as a function of time for the formation of the slip step. This time depends on dislocation velocities, and the latter depend on the effective stress or stress intensity factor. Thus, the authors manifested that they arrived at ‘the theoretical equation of SCC crack growth rate derived on the mechanochemical model’ for the crack strain rate as a function of the stress intensity factor. However, these equations show that the anodic dissolution rate here depends on the stress only through the dependence of the *number* of active planes on the stress, i.e., the authors took into account only a *quantity* of active sites as a function of stress during plastic slip (a purely mechanistic approach), but not the dependence of the “quality” of such planes on the stress that can be a true mechanochemical approach, which, first of all, should be based on the dependence of the chemical potential of the metal on the stress, as proposed in [19].

Besides, after the criticism of Gutman [51], the Ford–Andresen film rupture-dissolution model was again examined by Hall [52], and it was “concluded that the FA model cannot be considered either phenomenologically or fundamentally supported”. Therefore, selective dissolution of metal in the crack tip required for its growth may be caused by other reasons, which are not necessarily connected with competing processes of passive film rupture and recovering [51]. In this paper, we consider other possible processes that affect the dissolution of steel under stress (MCE) or mechanical behavior as a result of chemical/electrochemical interactions (CME) in a near-neutral pH aqueous medium, and, accordingly, the development of individual stages of SCC.

3. Mechanochemical and chemomechanical effects during SSC of pipe steels in pH-neutral aqueous media, taking into account the sequence of the process stages

It is generally recognized that the stress corrosion cracking of pipe steels is a multi-stage process, which includes at least four main stages: the incubation period, the initiation of cracks, the stable development of cracks to a critical size, and the accelerated accidental destruction [1,4,8,11,15,16, 53–57]. Let us consider the successive stages of the formation and propagation of the cracks from the point of view of the possible manifestation of the effects MCE and CME, using as an example the well-known scheme of the time-dependent crack velocity [1,4,8,49,54] (Figure 2), which are described in more detail in [15].

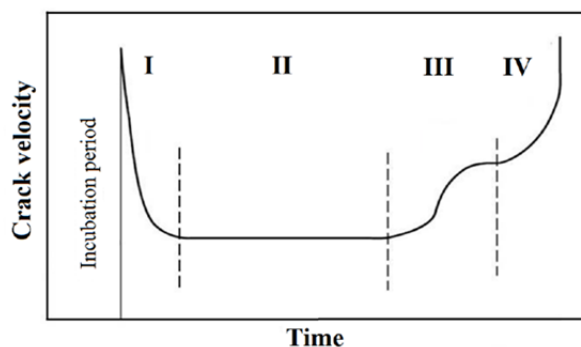


Figure 2. Schematic illustration of the effect of time upon SCC velocity (Reprinted with permission from Ref. [49]).

At stage 0 (the incubation period), metal dissolution, enhanced by stress and plastic deformation, occurs in NNpH solutions with the formation and growth of corrosive pits and “pitting-like” damage, formed near structural inhomogeneities (non-metallic inclusions, pearlitic colonies, slip bands, etc.) and near mechanical damage (scratches, dents or tears), which are stress concentrators on the surface of steel [8,11,55–60]. The key word here is “stress”, since the minimum of mechanochemical activity corresponds to zero stress. For example, for the samples of mechanically and electrochemically polished pure cobalt, the cathodic polarization curves in an acid electrolyte practically coincided. However, the anodic current densities at the same potential differed several times (up to 10) [61]. At close values of the degree of roughness, easier anodic dissolution is associated with residual stresses obtained by mechanical polishing. Increased corrosion of the metal caused by the simultaneous effects of stresses/deformations and the environment can be explained from the standpoint of the mechanochemical concept discussed above. Recently, some expressions of mechanochemistry, in particular, for the change of equilibrium electrode potential $\Delta\phi_0$ (Eqs 1 and 2) and anodic current density Δi_a (Eq 3) of elastically and plastically stressed metals, were taken into account in study of stress corrosion of pipeline steels in near-neutral pH solutions [29–32,59,60,62–64].

The effect of mechanical factors on parameters electrochemical reactions (MCE) appears, e.g., in the change in an open circuit potential (OCP) of pipe steels during the slow strain rate test in a 0.5M Na₂CO₃–1M NaHCO₃ solution [65] and in the NS4 (pH 6.8) anaerobic solution [62]. It was established that for X80 steel in a carbonate-bicarbonate solution open to air at the chosen strain rate ($1 \times 10^{-6} \text{ s}^{-1}$), OCP monotonically shifts in a positive direction at increasing strain from 0 to 0.070 due to the continuous formation of a passive film without its destruction even in the field of plastic deformation [60]. As contrary to this fact, in the NS4 anaerobic solution using the same strain rate and strain range, X70 steel shows the OCP shift to the negative direction with increasing strain. The effect of plastic deformation on the electrochemical parameters is attributed to three main aspects of MCE: an increase in the electrochemical thermodynamic activity of steel, a change in the density and distribution of dislocations, and an increase in surface roughness [59]. Similarly to [66,67], authors call the process of localized surface plasticity due to anodic dissolution which could increase the mobility of dislocations (CME) as “corrosion-facilitated plasticity” [60]. In this example, the close relationship between mechanochemical and chemomechanical effects is clearly manifested. Plastic deformation due to MCE causes a change in the electrochemical parameters (shift of an open circuit potential), contribute to the absorption and permeation of atomic hydrogen into steel, as well as

anodic dissolution, especially, in localized active centers, which serve as nucleation sites for cracks [68]; in turn, under certain conditions (low atomic hydrogen concentration, etc.), hydrogen can cause the hydrogen-induced plasticity (CME).

The effect of very small initial plastic deformation of X80 steel ranged from 0.001 to 0.008 (the yielding plateau) on corrosion behavior in 0.62 M NaCl was investigated in a four-point-loading apparatus in which the exact strain values were obtained using the adjustable bolt and measured by strain gauges [60]. Excluding a very narrow range of the strain (0.0055 ± 0.0010), the negligible values of i_{corr} were found which practically did not differ from that for unloaded samples. However, at strain closed to 0.0055, a six-fold increase in i_{corr} was observed. Such a jump in i_{corr} was explained by an avalanche increase in the number of dislocations (multiplication), which gradually turn into pile-ups of dislocations. Taking into account (Eq 2), the authors explain such a jump in i_{corr} by a significant increase in the number of dislocations n and resolved stress $\Delta\tau$, although the yield plateau is characterized by a constant value of $\Delta\tau$ [60]. Similar dependencies were obtained for the same steel in an in-situ tensile test combined with a potentiodynamic polarization test under the given potential (OCP + 100 mV) in a sulfate-reducing bacterial solution with $\text{pH} \approx 7.1$ [64]. At the beginning of the yielding plateau, a huge jump in Δi_a was detected from 0.18 to 10 μA due to destroying the dislocation pinning and their multiplication (a jump in n , see Eq 2). The further slight decrease of the anodic current density, as explain the author, is due to a decrease in the generation velocity of the Lüders bands (localized bands of plastic deformation in metals experiencing tensile stresses) [64]. The same phenomena have been observed in literature [19,31].

Mechanochemical behavior of X100 pipeline steel under uniaxial elastic stress in a near-neutral pH solution was estimated [30]. Take the relevant parameters and the maximum uniaxial stress of 600 MPa ($\sigma/\sigma_{\text{yield}} = 0.75$) into Eq 1, it was calculated that the theoretical change of equilibrium electrode potential is $\Delta\phi_0 = 7.4$ mV. The experiment showed that $\Delta\phi$ was significantly less than $\Delta\phi_0$. This is due to the significant electrochemical heterogeneity of the surface (places with predominant anodic or cathodic reactions), as a result of which the only average value of the electrode potential (OCP) is measured, while the Eq 1 refers to the local potential of the electrode, which varies much more significantly.

Additionally, when there is a local plastic deformation, the local corrosion activity is increased remarkably. With static elastic stress, which is well below the yield strength, local plastic deformation is possible, e.g., if there are some metallurgical defects, pits, etc. [19,31,63]. For example, when the solution contains an aggressive chlorine ion Cl^- , macroelastic deformation which is applied to bainitic and ferritic low carbon steels using both “soft” and “hard” loads (constant load and SSRT), respectively, causes stress accelerated corrosion due to MCE with pits formation [63]. When the critical stress exceeds 0.5 and 0.7 σ_{yield} for ferritic and bainitic steels, respectively, the applied mechanical energy will cause microplastic deformation of the macroelastic deformed steel, which generates at grain boundaries and then extends into the grains. Due to the stress concentration in the pits caused by chloride ion, the potential change $\Delta\phi$ under loading from 0 to 0.5 σ_{yield} was calculated to be 16.4 mV (Eq 1), which is smaller than the experimental value 33.8 mV. A large number of local plastic flows generated at grain boundaries due to enhanced dislocation motion are the reason which causes the break point in MCE [63]. In turn, additional anodic dissolution in regions of pits and grain boundaries is connected with local plastic deformation, and demonstrates manifestation of CME. However, the authors do not explain the reason why, at constant load, which exceeds the value of the critical stress, the corrosion current markedly decreases with an increase in

load for bainitic steel, and changes non-monotonously with increasing load for ferritic steel (a twofold growth with an increase in stress ratio from 0 to 0.3 $\sigma/\sigma_{0.2\%}$, then a three-fold decrease with increasing stress ratio from 0.3 to 0.5, etc.). This behavior of steels at constant load, which can be called “cold or room-temperature creep”, is unclear.

Potentiodynamic polarization of plastically deformed (pre-strained) samples [63] or specimens during a tensile test, e.g., SSRT [31,59,64,67], demonstrates increasing corrosion rate and crack growth rates due to MCE. It was showed that the influence of MCE becomes significant during plastic deformation of X100 steel [31]. The tests were carried out on the pre-strained X100 steel samples using the SSRT method ($1 \times 10^{-4} \text{ s}^{-1}$) in an NS4 solution at pH 6.8. Both anodic and cathodic reactions are enhanced at a pre-strain of 0.010, 0.022, and 0.039, however, its effect on anodic reaction is more significant. Plastic strain would increase the MCE significantly, as demonstrated by corrosion potential, coupling current density and electrochemical impedance spectroscopy (EIS) measurements. The authors suggest that, in reality, a non-uniform distribution of plastic stresses and strains on pipelines would cause quite different corrosion activities on the steel. This could be the reason to initiate preferential localized corrosion and even cracks [1,9]. On the base of a number of dependencies of mechanochemistry [17–19], the shift of electrochemical corrosion potential as a function of plastic strain, ε_{pl} , was established for the different initial density of dislocations N_0 prior to plastic deformation [31]. The calculation of the shift of corrosion potential shows that increasing N_0 on one order of magnitude from 1×10^8 to 1×10^9 at plastic deformation of 0.005 and 0.035 causes the shift of $\Delta\varphi_p^0$ in the negative direction from -4 to $-20 \text{ mV}_{\text{SCE}}$ and from -16 to $-42.5 \text{ mV}_{\text{SCE}}$, respectively. The indicated results on the assessment of dislocation densities, obtained by computational methods, require more detailed study and experimental confirmation in the case of SCC of pipe steels in media with a pH close to neutral.

According to [29], both the anodic and cathodic reactions should take into account at the analysis of the mechanochemical corrosion of plastically-strained steel. By FE method and using localized electrochemical impedance spectroscopy on the samples of X100 steel with various widths, it was shown quite different corrosion activities on the steel due to a non-uniform distribution of plastic strains. The FE simulation of MCE was performed using the pipe length segment of 2 m; the length of an elliptically shaped defect of 200 mm, and growing depths of 20%, 40%, 60% and 80% of the pipe wall thickness at constant length. The boundary conditions of solution: the solution boundary is electrically isolated, except the solution/steel interface that is set as a free boundary. The left end of the steel pipe is fixed; to simulate soil strain, the right end is loaded with tensile strain ranged from 0 to 0.004 along the longitudinal direction. The bottom of the pipe is set as electric grounding. The FE simulation included elasto-plastic solid stress analysis of the pipe, electrode potential and current density analysis at the steel/solution interface, and simulation and analysis of MCE, i.e., the interaction of mechanical parameters and electrochemical corrosion behavior of the steel in solution. The authors assume that the pipe steel is in an active dissolution state; as anodic reaction—dissolution of iron, and as cathodic reaction—reduction of H^+ ion to atomic hydrogen. The equilibrium potentials of anodic reaction depending on elastic and plastic strains were calculated using Eqs 1 and 2. Meantime, for describing of mechanochemical effect on cathodic reaction, a semi-empirical expression is derived, although the choice of such dependence is not quite clear:

$$i_c = i_{0,c} \cdot 10^{V_m \sigma_{Mises} / 6F(b_c)} \quad (5)$$

where $i_{0,c}$ is exchange current density of hydrogen evolution on X100 steel in the absence of external stress/strain, σ_{Mises} is von Mises stress calculated from FE, and b_c is cathodic Tafel slope [29].

The equilibrium potentials of the oxidation of steel and hydrogen evolution are determined by Nernst equations with the assumption that molecular hydrogen was adopted instead of atomic hydrogen reaction since the standard state of atomic hydrogen is not defined clearly. Assume the concentration of ferrous ions in NS4 solution is 10^{-6} M with solution pH of 6.8, the equilibrium potentials of anodic and cathodic half-reactions are calculated as -859 mV_{SCE} and -644 mV_{SCE}, respectively. The most important findings obtained using the FE model are the various effects of tensile strain and depth of corrosion defect on stress distribution. While tensile deformation leads to an overall increase of stress through the pipe wall, the increasing corrosion defect depth causes a more concentrated stress at the defect center, which serves as anode, and the sides of the defect, as cathode. Local plastic deformation due to increased tensile strain or the corrosion depth leads to anodic dissolution in the center of the defect, where local corrosion activity increases significantly.

Subsequently, this FE model was supplemented by the study of time-dependent mechanochemical effect at corrosion defect, enabling prediction of the defect growth over a long-term time period [32]. For example, anodic current density was calculated at the center of a stressed corrosion defect with initial depth of 2 mm over a period of up to 100 years depending on its width. The time dependence of local stress and anodic current density at corrosion defect can be featured with three stages, i.e., a negligible corrosion in elastic region; a slow increase of both stress and anodic current density under mild plastic deformation; and a rapid increase of both local stress and corrosion current density under a high local plastic deformation. The accelerated corrosion at stressed defects (MCE) can be mitigated effectively by reducing operating pressure and application of cathodic protection on pipelines. The disadvantage of this work [32] is the lack of consideration of residual stresses on the pipe surface. Thus, in [15], it was established that increased residual deformations measured by fiber-optic sensors when loading pipes with pressure are observed in areas with shallow corrosion defects and SCC cracks (depth up to 1.5 mm). Therefore, one should expect a high rate of steel dissolution even at small sizes of defects due to the influence of residual operational stresses in the surface layer.

A numerical method for studying mechanochemical processes in the pitting and grooving corrosion of steel structures under external and internal stresses was proposed [62]. FE analysis was performed for a $0.8 \times 0.8 \times 0.015$ m³ plate with pitting corrosion features and a simplified stiffened plate model ($4.75 \times 0.95 \times 0.015$ m³) with grooving corrosion features, as typical representatives of a deck or bottom plating of an oil tanker. Numerical simulation of these processes allows determining local surface areas with an increased level of stresses and deformations and, accordingly, identifying localized areas of accelerated dissolution of stressed metal (mechanochemical corrosion), and quantitatively describe the increase in dissolution current.

Modeling using the mechanochemical concept [29,32,62,64], allows one to predict the crack growth rate and current density of the anodic/cathodic reactions at local stress concentration, including corrosion defects on pipelines. However, based on such modeling, as a basic approach, new predictive models of SCC formation should be developed taking into account MCE and CME, as well as recommendations on the practical application of such modeling (or such models). Solving these problems will complement/improve the available material in accordance with the SCC prediction.

According to the analysis of the literature, we can certainly conclude that MCE plays a dominant role in the formation of pits, which are the sites of cracking. It is generally accepted that the main parameter determining the formation and rate of NNpHSCC microcracks (stage I) are the residual tensile stresses in the surface of pipes, the effect of which is added to the applied operational stresses and weakens as the depth of the crack increases [11,15,16]. As a result, the total tensile stresses on the surface of the pipe in places of local corrosion defects can reach the values of the yield strength of the material [69,70], and therefore the implementation of the CME and MCE is possible. It was found [71] a strong correlation between residual stress and the presence of near-neutral pH SCC colonies in pipes grades from X52 to X70. In a number of cases (as a first approximation), the effect of tensile residual stresses on SCC can be studied using constant loading in a corrosion solution. For example, in NS4 solution under the applied load σ_{appl} , which was very close to the yield strength $\sigma_{0.2\%}$, crack initiation was indeed observed in pipe steels X70 [72] and X80 [73]. As a result, during 278 d, the failure of steel X70 was observed at the stress ratio $\sigma_{\text{appl}}/\sigma_{0.2\%}$ of 0.999 for, while at the same duration and a ratio of 0.972 only pitting corrosion and cracks was observed without failure [72]. Similarly, during 148 d, the failure of X80 samples was revealed at $\sigma_{\text{appl}}/\sigma_{0.2} \geq 0.956$ [73].

The kinetics of further development of the SCC at this stage is determined by the aggressiveness of the near-pipe electrolyte, the level of residual stresses, structural and textural features in the surface layer of the pipe and to a lesser extent depends on the operational loads. The applied pipe manufacturing techniques lead to the formation on their surface of areas with different levels of residual deformation [69,70]. Reducing the effect of residual stresses [70,74] due to the textural heterogeneity of the material can lead to a partial or complete cessation of destruction [69,75]. Considering that the determination of the exact value of residual stresses in the metal of the pipe is difficult and requires further study, and the use of macro-properties of the material (mechanical characteristics) to describe the development of shallow (short) cracks is incorrect due to their variation even within one pipe [76], stage I requires more detailed study.

It appears that the chemomechanical effect can contribute in the process of crack formation on pipeline steels in neutral pH environments. For example, as indicated in [77], both atomic hydrogen and dissolution at the surface discontinuities can increase the surface plasticity of steel (micro-plastic deformation), contributing to crack initiation and propagation. At this time, as noted in [78], the emission of dislocations also plays an important role in promoting both localization of microplasticity and localized dissolution, as well as in maintaining crack sharpness.

The mechanism for the further development of NNpH cracks (stage II) is studied in the most detail. Most researchers are trying to explain the development of SCC at this stage by various interactions between applied stresses, hydrogenation and local metal dissolution. The influence of these processes on SCC is interrelated, and different authors point out on various combinations that have a dominant effect on crack growth.

The majority of researchers are trying to explain the propagation of SCC at this stage by the various interactions between hydrogen charging, and local dissolution of the metal [11,29,79–82]. It has been suggested [83–87] that hydrogen and cyclic loading plays a significant role in the cracking of pipeline steel in near-neutral pH electrolytes. As mechanisms of hydrogen influencing crack growth in NNpH solutions are considered hydrogen-induced plasticity (HIP) [88–96] and the internal-hydrogen-assisted cracking mechanism, instead of the hydrogen environmental-assisted cracking mechanism [87].

A large group of researchers believes that the cause of the growth of cracks in NNpHSCC pipe steels is the synergistic effect of anodic dissolution and hydrogen absorption in the metal [92,97,98]. A near neutral-pH environment is capable of generating a catalytic surface effect on hydrogen evolution in pipeline steels [99]. Hydrogen evolution markedly depends on the oxidation state of steels [100,101], and it changes the chemical potential of the steel and enhances anodic dissolution [102]. Thermodynamic justification of the effect of hydrogen concentration on anodic dissolution is given in [103–106]. Hydrogen introduced into the steel can promote anodic dissolution and SCC susceptibility, but these ideas contradict the known data on the inhibitory effect of atomic hydrogen on the anodic process of dissolution of iron in acidic environments [107].

It is important to note that the effect of hydrogen on the cracking of pipe steels manifests itself when it reaches a certain “critical” concentration in metal, which depends on the composition of the corrosive environment, as well as the type and level of the applied mechanical load [108]. However, it was established [109] that the current density of hydrogen penetration into steel in the field conditions does not reach the “critical” values, above which hydrogen embrittlement is observed. Therefore, the development of NNpHSCC with the predominant effect of absorbed hydrogen on crack growth is unlikely, but can be observed with a significant potential shift in the negative direction in solutions containing the hydrogen penetration promoter and/or under specific loading conditions (a certain combination of K , ΔK values and cycle frequency) [110–112].

Other researchers believe that local anodic dissolution of the metal has a major effect on crack growth in pipeline steel in weakly acidic and near-neutral electrolytes [15,79,113–116]. Selective dissolution of metal at the tip of the crack is not necessarily connected with competing processes of passive films rupture and recovering. Moreover, in NNpH solutions, conventional film rupture–repassivation theory does not apply for pipelines, which are in an active dissolution state [4]. However, as was recently proposed by Cheng [8], at an early stage of coating disbondment, the electrolyte penetrated under the coating is sufficiently thin and the steel can be in passivity. With an increase in the time and thickness of the solution layer, it is impossible to maintain the passivity of the steel, and the steel goes into the active state of dissolution. In our opinion, one of the possible reasons of cracking at this stage is the development of mechanochemical and chemomechanical effects at the tip of a crack. This conclusion is based on an analysis of the results presented below.

In work [117], the corrosion rate near the tip of previously grown fatigue cracks on X65 pipe steel samples was studied at various stress levels in a neutral pH medium (NS4 solution with 5% CO₂ purge to pH 6.6). It has been shown that near the tip of the crack, the steel is in a state of active dissolution. The corrosion potential near the tip of the unloaded crack was $-730 \text{ mV}_{\text{SCE}}$. There was no significant change in the values of corrosion potential (within $\pm 10\text{--}20 \text{ mV}$) near the crack tip under various loads. However, the current density of corrosion increased by more than 2 times with an increase in the applied load up to 95% of the yield strength of the steel, which indicates an increase in the corrosion rate near the crack tip and, as a result, the implementation of MCE.

The rate of local anodic dissolution of samples of ferritic-pearlite pipe made of steel X70 (yield strength of 650 MPa and tensile strength of 740 MPa) with pre-grown fatigue cracks (2–3 mm length) along the surface of the sample, as well as samples without cracks, was investigated under a constant load of 3000 N in NS4 solution, which was purged with 5% CO₂–N₂ to pH of 6.8 [118]. It has been established by numerical simulation methods that the stress concentration at the tip of the cracks reaches values up to 80% of the yield strength of steel when a tensile load of 3000 N is applied to samples with cracks. It is shown that such a stress concentration almost 3-fold increases the local

anodic dissolution rate of steel (and therefore MCE is implemented) at the crack tip. At the same time, the dissolution of the crack tip is accompanied by the formation of a layer of corrosion products on the metal surface, which does not effectively protect the steel from further dissolution due to a loose, porous structure. This leads to the continuous propagation of cracks and an increase in the concentration of stresses at the crack tip, which, in turn, further accelerates the local dissolution of the metal with the time of testing.

It has been suggested [8,81] that crack growth is possible through anodic plasticity caused by dissolution (CME), but this effect has not been studied in more detail. Another manifestation of the chemomechanical effect (in a wider sense than the definition given at the beginning of section 2) can be considered the results in [116]. It has been established that crack growth rate in X70 pipe steel in a weakly acid electrolyte (pH 5.5) under the action of a static load may slow down due to a decrease in the rate of dissolution of the metal with increasing degree of filling the surface with hydrogen. Thus, an indirect effect of the cathodic reaction of hydrogen evolution on the change in crack growth is shown, which can be considered as a special case of CME.

In works [88–96], the mechanism of crack growth was considered taking into account the concepts of hydrogen-induced plasticity (HIP). The effect of HIP can be considered as a special case of the CME. The HIP effect slows down the process of SCC of the steel in a near-neutral pH medium (NNpHSCC) due to an increase in the plastic deformation zone in front of the crack tip in the potential ranged from -680 to -930 mV_{SCE} (Figure 3) [67]. However, the detailed mechanism of HIP and its relationship to chemomechanical effect are unclear and require further study.

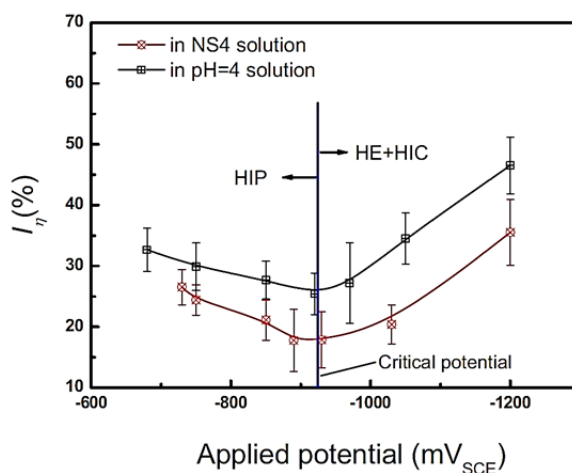


Figure 3. Effect of cathodic potential on reduction-in-elongation in NS4 solution and pH 4 solution as compared to air (Reprinted with permission from Ref. [67]).

Based on a detailed description of the reasons for the formation of SCC cracks in near neutral pH solutions, one can conclude that the main role in the process play residual stresses, but in our opinion, the more urgent issue is not the search for the causes of cracking (as stated above, these reasons have already been established), but how to take into account the quantitative contribution of these causes to the SCC process, for example, how to assess the influence of the level of residual deformations/stresses of pipes of various composition and strength classes for the intensity of electrochemical processes and the development of microcracks. For example, the empirical

expressions for describing the SCC speed at stages I and II proposed in [11] does not take into account the listed factors and can be used very approximately with the SCC forecast.

Further growth of the crack at stage III occurs with the participation of the near-pipe environment under design loads (seasonal ground movements, changes in working pressure), and is also determined by the interaction with adjacent cracks in the colony, with the result that when a certain size and relative position of the crack are reached, linear dimensions increase [8,54,55,119]. After that, an increasing effect of variable loads in the pipeline from gas pressure leads to the formation and development of a longitudinal main crack until the pipeline collapses. It can be assumed that at these stages of the process, the MCE is responsible for the accelerated anodic dissolution of the metal at the tip of a deep crack under the simultaneous action of the medium and variable load [120,121]. In addition, diffusion of atomic hydrogen to the tips of such cracks and the implementation, e.g., of hydrogen-induced cracking (HIC) [11,54] cannot be ruled out. Apparently, the qualitative laws governing the manifestation of MCE and CME at this stage will be similar to those discussed above, and quantifying the contribution of these effects will require taking into account the peculiarities of the variable loading.

4. Concluded remarks

An analysis of the literature has shown that the MCE and CME exist when cracking pipe steel. During the incubation period of a crack initiation near such inhomogeneities as grain boundaries, inclusions, metallurgical defects, etc., the dissolution of the metal, enhanced by stress during elastic and plastic deformation, takes place in NNpH solutions with formation and growth of corrosion pits, where undoubtedly, the MCE plays a dominant role. The MCE is responsible for accelerating anodic dissolution at the tip of a crack when a load is applied (constant or cyclic), which causes the crack to propagate. It has been shown that the MCE has been studied, including some examples of numerical modeling, in more detail than the CME. All authors agree that MCE accelerates the formation of corrosion defects and cracks propagation, however, the assessment of the quantitative contribution in the literature is either absent or controversial for different authors—the differences are associated primarily with different experimental conditions (sample shape, solution composition, loading conditions, etc.). It is obvious that studies of the CME during the cracking of pipe steels are few, isolated, and require further systematic study, including modeling. In the near future new methods of modeling both mechanochemical and chemomechanical effects should be developed for quantitative prediction of stress corrosion cracking in pipe steels.

In conclusion, it should be noted that further study of MCE and CME in the process of stress corrosion cracking of pipe steels requires more detailed experimental studies in the following areas:

- Determination of dislocation densities in pipe steels with SCC;
- Assessment of the influence of the level of residual deformations/stresses of pipes of different composition and strength classes on the intensity of electrochemical processes;
- Determination of the mechanisms of local dissolution of the metal at the tip of the crack, alternative to the generally accepted concepts of “film rupture-dissolution”;
- Assessment of the effect of atomic hydrogen on the plasticization of the surface layers at the tip of the crack;
- Determination of quantitative criteria to account for MCE and CME in a multi-stage model of pH-neutral SCC pipe steels.

Conflict of interests

All authors declare no conflicts of interest in this paper.

References

1. National Energy Board (1996) Public inquiry concerning stress corrosion cracking on Canadian oil and gas pipelines: report of the inquiry. MH-2-95, Canada.
2. Canadian Energy Pipeline Association (1996) Submission to the National Energy Board. *Proceeding MH-2-95*, 2.
3. Gareev AG, Ivanov IA, Abdullin IG, et al. (1997) *Prognozirovaniye Korroziionno-Mekhanicheskikh Razrusheniy Magistral'nykh Truboprovodov (Prediction of Corrosion/Mechanical Damage to Main Pipelines)*, Moscow: Gazprom IRZ, 1–170. (in Russian)
4. Parkins R (2000) A review on SCC of high-pressure pipelines. *NACE-International Corrosion Conference Series*, 00363.
5. Arabey AB, Knoshinski Z (2006) *Korroziionnoe Rastreskivanie Pod Napryazheniem Trub Magistral'nykh Gazoprovodov. Atlas (Stress Corrosion Cracking of Main Gas Pipelines. Atlas)*, Moscow: Nauka, 1–106. (in Russian)
6. King F (2010) Stress corrosion cracking of carbon steel used fuel containers in a Canadian deep geological repository in sedimentary rock. TR-2010-21, Nuclear Waste Management Organization, 34.
7. Meresht ES, Farahani TS, Neshati J (2011) Failure analysis of stress corrosion cracking occurred in a gas transmission steel pipeline. *Eng Fail Anal* 18: 963–970.
8. Cheng YF (2013) *Stress Corrosion Cracking of Pipelines*, Hoboken: John Wiley & Sons, 257.
9. Alimov SV, Arabey AB, Ryakhovskikh IV, et al. (2015) The concept of diagnosis and repair gas mains in regions with high susceptibility to stress corrosion cracking. *Nat Gas Indust* 724: 10–15. (in Russian)
10. Gamboa E (2015) Inclined stress corrosion cracks in steel pipelines. *Corros Eng Sci Technol* 50: 191–195.
11. Chen W (2016) An overview of near-neutral pH stress corrosion cracking in pipelines and mitigation strategies for its initiation and growth. *Corrosion* 72: 962–977.
12. Canadian Energy Pipeline Association (CEPA) (2015) *Recommended Practices for Managing Near-neutral pH Stress Corrosion Cracking 3rd Edition*, 158. Available from: https://www.cepa.com/wp-content/uploads/2016/11/Stress-Corrosion-Cracking_3rdEdition_CEPA_FINAL.pdf
13. Malkin AI, Marshakov AI, Arabey AB (2009) Processes of crack initiation and propagation on the steels of main pipelines. Part I: modern understanding of the mechanisms of stress corrosion cracking of pipeline steels in aqueous media. *Corros Mater Prot* 10: 1–16.
14. Parkins RN, Blanchard WK, Delanty BS (1994) Transgranular stress corrosion cracking of high-pressure pipelines in contact with solutions of near neutral pH. *Corrosion* 50: 394–408.
15. Ryakhovskikh IV, Bogdanov RI, Arabey AB (2019) Regularities of pipelines stress corrosion cracking. *14th Pipeline Technology Conference*, 1–13.

16. Ryakhovskikh IV, Bogdanov RI, Rodionova IG et al. (2018) Regularities of stress corrosion cracking of pipe steels. *9th Eurasian Scientific and Practical Conference "Strength of Heterogeneous Structures-PROST 2018"*, 191. (in Russian)
17. Gutman EM (1967) A transl. of Fiziko-khimicheskaya mekhanika materialov, Academy of Sciences of the Ukrainian SSR. *Sov Mat Sci* 3: 190–196, 304–310, 401–409.
18. Gutman EM (1974) *Mechanochemistry of Metals and Corrosion Prevention*, Moscow: Metallurgy, 231. (in Russian)
19. Gutman EM (1994) *Mechanochemistry of Solid Surfaces*, New Jersey-London-Singapore: World Scientific, 332.
20. Gutman EM (1998) *Mechanochemistry of Materials*, Cambridge: Cambridge Interscience, 205.
21. Gutman EM (1994) Surface plasticity modification using electrolytic etching. *Surf Coat Tech* 67: 133–136.
22. Ostwald W (1917) *Grundriss der allgemeinen Chemie*, 5 Eds., Dresden: Steinkopff.
23. Heinicke G (1984) *Tribochemistry*, Berlin: Akademie-Verlag.
24. Boldyrev VV (1983) Experimental methods in mechanochemistry of inorganic solids, In: Herman H, *Treatise on Materials Science and Technology*, New York: Academic Press, 19: 185–223.
25. Butyagin PY (1989) *Active States in Mechanochemical Reactions*, Glasgow: Harwood Academic Publishers.
26. Tkacova K (1989) *Mechanical Activation of Minerals*, Amsterdam: Elsevier.
27. Suryanarayana C (2001) Mechanical alloying and milling. *Prog Mater Sci* 46: 1–184.
28. Baláz P (2008) *Mechanochemistry in Nanoscience and Minerals Engineering*, Berlin: Springer-Verlag, 413.
29. Xu LY, Cheng YF (2013) Development of a finite element model for simulation and prediction of mechano-electrochemical effect of pipeline corrosion. *Corros Sci* 73: 150–160.
30. Xu LY, Cheng YF (2012) An experimental investigation of corrosion of X100 pipeline steel under uniaxial elastic stress in a near-neutral pH solution. *Corros Sci* 59:103–109.
31. Xu LY, Cheng YF (2012) Corrosion of X100 pipeline steel under plastic strain in a neutral pH bicarbonate solution. *Corros Sci* 64: 145–152.
32. Xu LY, Cheng YF (2017) A finite element based model for prediction of corrosion defect growth on pipelines. *Int J Pres Ves Pip* 153: 70–79.
33. Oura K, Lifshits VG, Saranin AA, et al. (2003) *Surface Science-An Introduction*, New York: Springer-Verlag, 440.
34. Gutman EM, Fourie JT (1977) *Surface Effects in Crystal Plasticity*, Netherlands: Springer, 17: 737.
35. Cottrell AH, Bilby BA (1949) Dislocation theory of yielding and strain ageing of iron. *Proc Phys Soc Sec A* 62: 49–62.
36. Dieter GE (2000) Mechanical behavior under tensile and compressive loads, In: Medlin A, *Mechanical Testing and Evaluation*, ASM International, 8: 237–262.
37. Guo XH, Lu BT, Luo JL (2006) Responce of surface mechanical properties to electrochemical dissolution determined by in situ nanoindentation technique. *Electrochem Commun* 8: 1092–1098.
38. Gutman EM, Unigovski Ya, Shneck R, et al. (2016) Electrochemically enhanced surface plasticity of steels. *Appl Surf Sci* 388: 49–56.

39. Zhu RK, Lu BT, Luo JL, et al. (2013) Effect of cold work on surface reactivity and nano-hardness of alloy 800 in corroding environment. *Appl Surf Sci* 270: 733–762.
40. Revie RW, Uhlig H (1974) Effect of applied potential and surface dissolution on the creep behavior of copper. *Acta Metall* 22: 619–627.
41. Olive JM, Sarrazin C (1993) Effect of anodic dissolution on creep rate of austenitic stainless steel, *Corrosion-Deformation Interactions*, In: Magnin T, Gras JM, France: Les Editions de Physique, 153–162.
42. Unigovski Ya, Keren Z, Eliezer A, et al. (2005) Creep behavior of pure magnesium and Mg–Al alloys in active environments. *Mater Sci Eng A* 398: 188–197.
43. Unigovski Ya, Gutman EM (2011) Corrosion creep and fatigue behavior of Mg alloys, *Corrosion of Magnesium Alloys*, In: Song GL, Oxford-Cambridge-Philadelphia-New Delhi: Woodhead Publishing, 365–402.
44. Hoar TP, West JM (1962) Mechano-chemical anodic dissolution of austenitic stainless steel in hot chloride solution. *Proc R Soc London Ser A* 268: 304–315.
45. Raicheff RG, Damjanovic A, Bockris JO'M (1967) Dependence of the velocity of the anodic dissolution of iron on its yield rate under tension. *J Chem Phys* 47: 2198–99.
46. Despic AR, Raicheff RG, Bockris JO'M (1968) Mechanism of the acceleration of the electrodic dissolution of metals during yielding under stress. *J Chem Phys* 49: 926–938.
47. Scully JC (1975) Stress corrosion crack propagation: A constant charge criterion. *Corros Sci* 15: 207–224.
48. Andresen PL, Ford FP (1988) Life prediction by mechanistic modeling and system monitoring of environmental cracking of iron and nickel alloys in aqueous systems. *Mater Sci Eng A* 103: 167–184.
49. Parkins RN (1988) Localized corrosion and crack initiation. *Mater Sci Eng A* 103: 143–156.
50. Saito K, Kunya J (2001) Mechanochemical model to predict SCC growth of stainless steel in high temperature water. *Corros Sci* 43: 1751–1766.
51. Gutman EM (2007) An inconsistency in “film rupture model” of stress corrosion cracking. *Corros Sci* 49: 2289–2302.
52. Hall JR, MM (2009) Critique of the Ford–Andresen film rupture model for aqueous stress corrosion cracking. *Corros Sci* 51: 1103–1106.
53. Chen W, King F, Vokes E (2002) Characteristics of near-neutral-pH stress corrosion cracks in an X-65 pipeline. *Corrosion* 58: 267–275.
54. Chen W (2017) Modeling and prediction of stress corrosion cracking of pipeline steels, In: El-Sherik AM, *Trends in Oil and Gas Corrosion Research and Technologies Production and Transmission*, France: Woodhead Publishing, 707–748.
55. Ryakhovskikh IV (2013) A complex technique of research of corrosion-mechanical properties of low-carbon low-alloyed pipe steels and an assessment of their firmness against SCC [PhD's thesis]. National Research Nuclear University MEPhI, Moscow, 155. (in Russian)
56. Wang SH, Chen W, King F, et al. (2002) Precyclic-loading-induced stress corrosion cracking of pipeline steels in a near-neutral-pH soil environment. *Corrosion* 58: 526.
57. Chu R, Chen W, Wang SH, et al. (2004) Microstructure dependence of stress corrosion cracking initiation in X65 pipeline steel exposed to a near-neutral pH soil environment. *Corrosion* 60: 275.

58. Viktorovich RI, Esiev TS, Kohtev SA (2012) Improving methods of estimating the propensity of pipeline steels to stress corrosion cracking. *Phys Chem Mater Processing* 4: 88–93. (in Russian)
59. Cui Z, Liu Z, Wang L, et al. (2016) Effect of plastic deformation on the electrochemical and stress corrosion cracking behavior of X70 steel in near-neutral pH environment. *Mater Sci Eng A* 677: 259–273.
60. Wang Y, Zhao W, Ai H, et al (2011) Effects of strain on the corrosion behavior of X80 steel. *Corros Sci* 53: 2761–2766.
61. Talbot DEJ, Talbot JDR (1997) Corrosion science and technology, 1 Ed., *Materials Science & Technology*, New York: CRC-Press, 406.
62. Wang Y, Wharton JA, Shenoi RA (2016) Mechano-electrochemical modelling of corroded steel structures. *Eng Struct* 128: 1–14.
63. Ren RK, Zhang S, Pang XL, et al. (2012) A novel observation of the interaction between the macroelastic stress and electrochemical corrosion of low carbon steel in 3.5 wt% NaCl solution. *Electrochim Acta* 85: 283–294.
64. Wu T, Yan M, Xu J, et al. (2016) Mechano-chemical effect of pipeline steel in microbiological corrosion. *Corros Sci* 108: 160–168.
65. Zhao W, Zou Y, Xia DX, et al. (2015) Effects of anodic protection on SCC behavior of X80 pipeline steel in high-pH carbonate-bicarbonate solution. *Arch Metall Mater* 60: 1009–1013.
66. Lu BT, Luo JL, Norton PR (2010) Environmentally assisted cracking mechanism of pipeline steel in near-neutral pH groundwater. *Corros Sci* 52: 1787–1795.
67. Liu ZY, Wang XZ, Du CW, et al. (2016) Effect of hydrogen-induced plasticity on the stress corrosion cracking of X70 pipeline steel in simulated soil environments. *Mater Sci Eng A* 658: 348–354
68. Bueno AHS, Castro BB, Ponciano JAC (2008) Assessment of stress corrosion cracking and hydrogen embrittlement susceptibility of buried pipeline steels, In: Shipilov SA, Jones RH, Olive J-M, et al., *Environment-Induced Cracking of Materials*, 2 Eds., Elsevier, 2: 313–322.
69. Perlovich YA, Ryakhovskikh IV, Isaenkova MG, et al. (2017) Correlation between the resistance to stress corrosion cracking of steel tubes of gas pipelines with their layerwise texture inhomogeneity. *KnE Mater Sci* 179–186.
70. Arabey AB, Esiyev TS, Ryakhovskikh IV, et al. (2012) Influence of features of the pipe production technology on resistance to stress corrosion cracking during the operation of main gas pipelines. *The Gas Industry*, 2: 52–54. (in Russian)
71. Beavers JA, Johnson JT, Sutherby RL (2000) Materials factors influencing the initiation of near-neutral pH SCC on underground pipelines. *2000 International Pipeline Conference* 2: 979–998.
72. Fang BY, Han EH, Wang JQ, et al. (2013) Stress corrosion cracking of X-70 pipeline steel in near neutral pH solution subjected to constant load and cyclic load testing. *Corros Eng Sci Techn* 42: 123–129.
73. Jia YZ, Wang JQ, Han EH, et al. (2011) Stress corrosion cracking of X80 pipeline steel in near-neutral pH environment under constant load tests with and without preload. *J Mater Sci Techn* 27: 1039–1046.
74. Masoumi M, Abreu H (2015) Textural analysis through thickness of API X70 steel after hot rolling and post heat treatment. *The Brazilian Materials & Mining Association*, 52: 1–10.

75. Pyshmintsev I, Gervasyev A, Petrov RH, et al. (2012) Crystallographic texture as a factor enabling ductile fracture arrest in high strength pipeline steel. *Mater Sci Forum* 702–703: 770–773.
76. Lyakishev NP, Kantor MM, Voronin VN et al. (2005) The study of the metal structure of gas pipelines after their long operation. *Metally* 1: 3–16. (In Russian)
77. Lu BT, Luo JL, Norton PR (2010) Environmentally assisted cracking mechanism of pipeline steel in near-neutral pH groundwater. *Corros Sci* 52: 1787–1795.
78. Elboudjaini M, Wang YZ, Revie RW, et al (2000) Stress corrosion crack initiation processes: pitting and microcrack coalescence. *NACE-International Corrosion Conference Series*, 00379.
79. Lu BT, Luo JL, Norton PR, et al. (2009) Effects of dissolved hydrogen and elastic and plastic deformation on active dissolution of pipeline steel in anaerobic groundwater of near-neutral pH. *Acta Mater* 57: 41–49.
80. Tang X, Cheng YF (2011) Quantitative characterization by micro-electrochemical measurements of the synergism of hydrogen, stress and dissolution on near-neutral pH stress corrosion cracking of pipelines. *Corros Sci* 53: 2927–2933.
81. Marshakov AI, Ignatenko VE, Bogdanov RI, et al. (2014) Effect of electrolyte composition on crack growth rate in pipeline steel. *Corros Sci* 83: 209–216.
82. Egbewande A, Chen W, Eadie R, et al. (2014) Transgranular crack growth in the pipeline steels exposed to near-neutral pH soil aqueous solutions: discontinuous crack growth mechanism. *Corros Sci* 83: 343–354.
83. Chen W, Kania R, Worthingham R, et al. (2009) Transgranular crack growth in the pipeline steels exposed to near-neutral pH soil aqueous solutions: the role of hydrogen. *Acta Mater* 57: 6200–6214.
84. Asher SL, Singh PM (2009) Role of stress in transgranular stress corrosion cracking of transmission pipelines in near-neutral pH environments. *Corrosion* 65: 79–87.
85. Lu BT, Luo JL, Norton PR (2010) Environmentally assisted cracking mechanism of pipeline steel in near-neutral pH groundwater. *Corros Sci* 52: 1787–1795.
86. Wang R (2009) Effects of hydrogen on the fracture toughness of a X70 pipeline steel. *Corros Sci* 51: 2803–2810.
87. Kang Y, Chen W, Kania R, et al. (2011) Simulation of crack growth during hydrostatic testing of pipeline steel in near-neutral pH environment. *Corros Sci* 53: 968–975.
88. Chu WY, Hsiao CM, Li SQ (1979) Hydrogen induced delayed plasticity and cracking. *Scr Metall* 13: 1063–1068.
89. Robertson IM, Birnbaum HK (1986) An HVEM study of hydrogen effects on the deformation and fracture of nickel. *Acta metall* 34: 353–366.
90. Rozenak P, Robertson IM, Birnbaum HK (1990) HVEM studies of the effects of hydrogen on the deformation and fracture of AISI type 316 austenitic stainless steel. *Acta Metall Mater* 38: 2031–2040.
91. Delafosse D, Magnin T (2001) Hydrogen induced plasticity in stress corrosion cracking of engineering systems. *Eng Fract Mech* 68: 693–729.
92. Lu BT, Luo JL (2008) A mechanistic study on near-neutral pH stress corrosion cracking of pipeline steel, In: Shipilov SA, Jones RH, Olive J-M, et al., *Environment-Induced Cracking of Materials*, Elsevier, 2: 243–253.

93. Lynch SP (2008) Towards understanding the mechanisms and kinetics of environmentally assisted cracking. In: Shipilov SA, Jones RH, Olive J-M, et al., *Environment-Induced Cracking of Materials*, Elsevier, 1: 167.
94. Kishore R (2009) Effect of hydrogen on the creep behavior of Zr–2.5% Nb alloy at 723K. *J Nucl Mater* 385: 591–594.
95. Barnoush A, Zamanzade M, Vehoff H (2010) Direct observation of hydrogen-enhanced plasticity in super duplex stainless steel by means of in situ electrochemical methods. *Scr Mater* 62: 242–245.
96. Dmytrakh IM, Leshchak RL, Syrotyuk AM, et al. (2017) Effect of hydrogen concentration on fatigue crack growth behaviour in pipeline steel. *Int J Hydrogen Energ* 42: 6401–6408.
97. Delafosse D, Bayle B, Bosch C (2008) The roles of crack-tip plasticity, anodic dissolution and hydrogen in SCC of mild and C–Mn steels. In: Shipilov SA, Jones RH, Olive J-M, et al., *Environment-Induced Cracking of Metals*, Elsevier, 2: 267–278.
98. Been J, King F, Sutherby RL (2008) Environmentally assisted cracking of pipeline steels in near-neutral pH environments. In: Shipilov SA, Jones RH, Olive J-M, et al., *Environment-Induced Cracking of Metals*, Elsevier, 2: 221–230.
99. Niu L, Cheng YF (2007) Corrosion behavior of X-70 pipe steel in near-neutral pH solution. *Appl Surf Sci* 253: 8626–8631.
100. Flis J, Zakroczymski T (1992) Enhanced hydrogen entry in iron at low anodic and low cathodic polarizations in neutral and alkaline solutions. *Corrosion* 48: 530–539.
101. King F, Jack T, Chen W, et al. (2000) Mechanistic studies of initiation and early stage crack growth for near-neutral pH SCC on pipelines. *NACE-International Corrosion Conference Series*, 00361.
102. Li MC, Cheng YF (2007) Mechanistic investigation of hydrogen-enhanced anodic dissolution of X-70 pipe steel and its implication on near-neutral pH SCC of pipelines. *Electrochim Acta* 52: 8111–8117.
103. Qiao L, Mao X (1995) Thermodynamic analysis on the role of hydrogen in anodic stress corrosion cracking. *Acta Metall Mater* 43: 4001–4006.
104. Qiao LJ, Luo JL, Mao X (1997) The role of hydrogen in the process of stress corrosion cracking of pipeline steels in dilute carbonate-bicarbonate solution. *J Mater Sci Lett* 16: 516–520.
105. Mao SX, Li M (1998) Mechanics and thermodynamics on the stress and hydrogen interaction in crack tip stress corrosion: experiment and theory. *J Mech Phys Solids* 46:1125–1137.
106. Gu B, Luo J, Mao X (1999) Hydrogen-facilitated anodic dissolution-type stress corrosion cracking of pipeline steels in near-neutral pH solution. *Corrosion* 55: 96–106.
107. Marshakov AI, Maleeva MA, Rybkina AA et al. (2010) Effect of atomic hydrogen on the anodic dissolution of iron in a weakly acidic sulfate electrolyte. *Prot Met Phys Chem* 46: 40–49.
108. Ignatenko VE, Marshakov AI, Marichev VA, et al. (2000) Effect of cathodic polarization on the corrosion cracking rate in pipe steels. *Prot Met Phys Chem* 36: 111–117.
109. Mikhailovsky YuN, Marshakov AI, Ignatenko VE et al. (2000) Estimation of the probability of hydrogen embrittlement of steel gas pipelines in the action areas of cathode stations. *Prot Met Phys Chem* 36: 140–145.
110. Ignatenko VE, Kuznetsov YuI, Arabei AB, et al. (2013) Application of SSRT to estimate the effect of corrosive medium on the liability of X70 pipe steel to stress corrosion cracking. *Int J Corros Scale Inhib* 2: 318–336.

111. Bogdanov RI (2013) Regularities of stress corrosion cracking of a X70 pipe steel in near-neutral pH ground electrolytes [PhD's thesis]. A.N. Frumkina RAS, Moscow, 201. (in Russian)
112. Marshakov AI, Ignatenko VE, Bogdanov RI, et al. (2014) Effect of electrolyte composition on crack growth rate in pipeline steel. *Corros Sci* 83: 209–216.
113. Arabey AB, Bogdanov RI, Ignatenko VE, et al. (2011) Effect of corrosion medium composition on rate of crack growth in X70 pipeline steel. *Prot Met Phys Chem* 47: 236–244.
114. Bogdanov RI, Marshakov AI, Ignatenko VE (2011) Effect of solution composition on crack growth rate in X70 pipeline steel under static and cyclic loading. *Corros Mater Prot* 11: 30–38 (In Russian)
115. Ryakhovskikh IV, Bogdanov RI, Esiev TS, et al. (2014) Stress corrosion cracking of pipeline steel in near-neutral pH environment. *Materials Science and Technology Conference and Exhibition*, 2: 807–814.
116. Bogdanov RI, Marshakov AI, Ignatenko VE, et al. (2017) Effect of hydrogen peroxide on crack growth rate in X70 pipeline steel in weak acid solution. *Corros Eng Sci Techn* 52: 294–301.
117. Yang Y, Cheng YF (2016) Stress enhanced corrosion at the tip of near-neutral pH stress corrosion cracks on pipelines. *Corrosion* 72: 1035–1043.
118. Tang X, Cheng YF (2009) Micro-electrochemical characterization of the effect of applied stress on local anodic dissolution behavior of pipeline steel under near-neutral pH condition. *Electrochim Acta* 54: 1499–1505.
119. Malkin AI, Marshakov AI, Ignatenko VE, et al. (2010) Processes of crack initiation and propagation on the steels of main pipelines. Part II. The kinetics of crack growth and environmental effects on SCC of pipeline steels in aqueous media. *Corros Mater Prot* 2: 1–11.
120. Zhao W, Xin R, He Z, et al. (2012) Contribution of anodic dissolution to the corrosion fatigue crack propagation of X80 steel in 3.5 wt% NaCl solution. *Corros Sci* 63: 387–392.
121. Cui ZY, Liu ZY, Wang XZ, et al. (2016) Crack growth behaviour and crack tip chemistry of X70 pipeline steel in near-neutral pH environment. *Corros Eng Sci Techn* 51: 352–357.



AIMS Press

© 2019 the Author(s), licensee AIMS Press. This is an open access article distributed under the terms of the Creative Commons Attribution License (<http://creativecommons.org/licenses/by/4.0>)